Role of Antisite Disorder on Preamorphization Swelling in Titanate Pyrochlores

Y. H. Li,[1,2] B. P. Uberuaga,[1] C. Jiang,[1,3] S. Choudhury,[1] J. A. Valdez,[1] M. K. Patel,[1] J. Won,[1] Y.-Q. Wang,[1] M. Tang,[1] D. J. Safarik,[1] D. D. Byler,[1] K. J. McClellan,[1] I. O. Usov,[1] T. Hartmann,[4] G. Baldinozzi,[5] and K. E. Sickafus[1,6,*]

[1]*Materials Science and Technology Division, Los Alamos National Laboratory, Los Alamos, New Mexico 87545, USA*
[2]*School of Nuclear Science and Technology, Lanzhou University, Lanzhou, 7340000, China*
[3]*Department of Materials Science and Engineering, University of Wisconsin, Madison, Wisconsin 53705, USA*
[4]*Harry Reid Center for Environmental Studies, University of Nevada—Las Vegas, Las Vegas, Nevada 89154-4009, USA*
[5]*Structures, Propriétés et Modélisation des Solides, CNRS UMR 8580, Ecole Centrale Paris, 92295 Châtenay-Malabry, France*
[6]*Department of Materials Science and Engineering, The University of Tennessee, Knoxville, Tennessee 37996, USA*

(Received 12 April 2011; published 8 May 2012)

Ion irradiation experiments and atomistic simulations were used to demonstrate that irradiation-induced lattice swelling in a complex oxide, $Lu_2Ti_2O_7$, is due initially to the formation of cation antisite defects. X-ray diffraction revealed that cation antisite formation correlates directly with lattice swelling and indicates that the volume per antisite pair is approximately 12 Å^3. First principles calculations revealed that lattice swelling is best explained by cation antisite defects. Temperature accelerated dynamics simulations indicate that cation Frenkel defects are metastable and decay to form antisite defects.

DOI: 10.1103/PhysRevLett.108.195504 PACS numbers: 61.72.Bb, 61.72.Dd, 61.72.J−

Swelling of crystalline solids due to radiation damage is a phenomenon of both scientific and practical importance. Changes in unit cell lattice parameters in silicates have been attributed to interstitials (expansion), vacancies (contraction), and reorientation of the SiO_4 tetrahedra (expansion) [1]. In general, however, the contributions of defects to lattice swelling are not well understood.

Johannson and Linde in 1936 [2] were the first to correlate atomic disorder with lattice swelling, specifically in Cu-Au intermetallic alloys. In the case of complex oxides, there have been numerous studies of atomic disordering phenomena, including published reports on disordering in the pyrochlore oxide, $Lu_2Ti_2O_7$, which is the subject of this Letter. Disordering studies on $Lu_2Ti_2O_7$ include thermally induced disorder [3–7] and radiation-induced disorder [8,9].

The purpose of this Letter is to demonstrate two findings: (1) experimental evidence for a correlation between irradiation-induced atomic disorder and lattice swelling in a ceramic oxide pyrochlore-structured compound, $Lu_2Ti_2O_7$ (hereafter referred to as LTO); and (2) theoretical evidence for the nature of the defects responsible for this swelling. The lattice swelling observed here ($\sim$ 6–8 vol.%) is ultimately more than an order of magnitude larger than in the intermetallics described above. It will be demonstrated that the defect responsible for the swelling is the *antisite* defect. Antisite defects occur in pyrochlore when atoms on one sublattice exchange positions with atoms on the other to form sublattice atomic defects, $A_A + B_B \rightarrow A_B + B_A$, where $A_B + B_A$ is an antisite pair (the subscripts "A" and "B" represent the A and B cation sublattices in $A_2B_2O_7$ pyrochlore).

Polycrystalline, monophasic samples of LTO were prepared by mixing end-member oxide powders (99.99% purity Lu_2O_3 and 99.9% purity TiO_2) and sintering at high temperature in air to obtain pellets with $\sim$90% density. Cut and polished disks from these pellets were irradiated with 400 keV Ne^{2+} ions at cryogenic temperature ($\sim$ 77 K), using a 200 kV Danfysik ion implanter in the Ion Beam Materials Laboratory at Los Alamos National Laboratory. Ne ions were used to minimize or eliminate in-cascade amorphization, while accentuating simple, point defect accumulation mechanisms. Samples were irradiated at normal incidence to fluences from 1×10^{18} to 1×10^{20} Ne/m^2 with a flux of $\sim 1 \times 10^{16}$ Ne/m$^2 \cdot$ s. The projected range of the Ne ions in LTO is approximately 470 nm and the peak in the damage distribution is at a depth of $\sim$330 nm (based on the stopping and range of ions in matter (SRIM) simulations [10], using 40 eV for the displacement threshold for all atomic species). LTO samples were examined before and after irradiation using grazing incidence x-ray diffraction (GIXRD; measurements made using Cu K_α radiation in θ–2θ geometry, over an angular range, $10° \leq 2\theta \leq 80°$ at an incidence angle of 0.25°, which probes a sample depth of <50 nm). GIXRD peaks were fit with pseudo-Voigt peak shapes [11] to determine the centroid, 2θ, position of each peak and peak intensities (following background subtraction). Peak positions were converted to interplanar lattice spacings, d, using Bragg's Law [11].

Density functional theory (DFT) calculations of defect energies and volumes in LTO were performed using VASP [12–14] applying the projector augmented wave method [15] using a 500 eV plane wave cutoff and a $2 \times 2 \times 2$ k-point sampling of the Brillouin zone. Calculations were done on 88-atom cells and atomic positions and cell volumes and shapes were relaxed. No symmetry constraints were imposed in these calculations. All calculations were converged until the maximum force on any atom

was less than 0.05 eV/Å, though typically significantly better. Temperature accelerated dynamics (TAD) [16] was used to simulate the recombination of Frenkel pairs in LTO, using a Buckingham potential [17,18]. The TAD simulations were performed on systems containing 704 atoms (a $2 \times 2 \times 2$ supercell) with a low temperature of 2000 K. Simulation times ranged from 5 to 800 ns.

Two phenomena were revealed upon comparing pristine versus irradiated LTO GIXRD patterns. First, the LTO interplanar lattice spacings increased with increasing dose. Second, with increasing dose, the intensities of the *pyrochlore* "superlattice" x-ray reflections diminished relative to the intensities of the "fundamental" x-ray reflections associated with the parent, *fluorite* crystal structure [19]. Figure 1 shows GIXRD patterns obtained at an x-ray incidence angle of 0.25°, illustrating both phenomena. First, Fig. 1 shows the gradual shift of reflections such as the {222} reflection to lower scattering angles, 2θ, with increasing fluence (or dose). Second, one can also discern the gradual diminishing in the intensity of the {111} reflection, a pyrochlore superlattice reflection, relative to the intensity of the {222} fundamental fluorite reflection, again with increasing fluence. The shift of the lattice reflections to smaller 2θ indicates unit cell swelling: the lattice parameter, a, increases. Diminishing superlattice reflection intensity is primarily indicative of cation disordering, the formation of antisites (Lu_{Ti} and Ti_{Lu} defects) [20]. The degree of antisite disorder can be quantified using the inversion parameter, i (see the Supplemental Material [21]). Table I summarizes changes in a and in the intensity ratio, $I\{111\}/I\{222\}$, as a function of ion fluence.

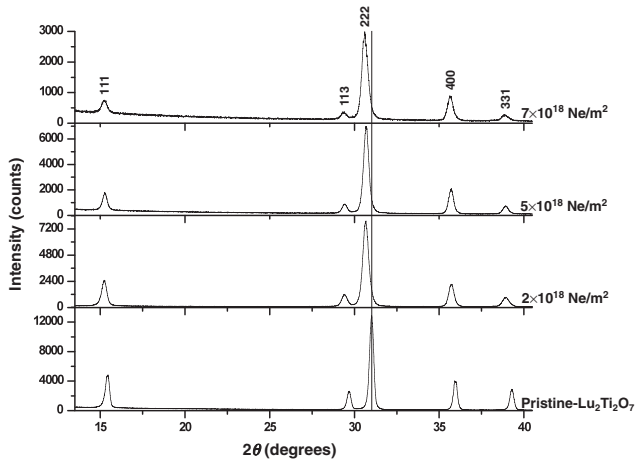

FIG. 1. Grazing incidence x-ray diffraction (GIXRD) patterns obtained from four $Lu_2Ti_2O_7$ samples (from bottom to top): (1) pristine (unirradiated) $Lu_2Ti_2O_7$ and $Lu_2Ti_2O_7$ irradiated to fluences of (2) 2×10^{18} Ne/m^2, (3) 5×10^{18} Ne/m^2, and (4) 7×10^{18} Ne/m^2. The {111}, {113}, and {331} peaks are pyrochlore superlattice reflections, while the {222} and {400} peaks are fundamental, fluorite reflections. The line through the pristine {222} reflection shows that the irradiated reflections are shifted to lower scattering angles, 2θ.

The calculated intensity ratio, $I\{111\}/I\{222\}$, for an ideal, fully ordered ($i = 0$) LTO pyrochlore is 0.36156. Table I indicates that the GIXRD measured value for the pristine LTO sample is $I\{111\}/I\{222\}|_{\text{pristine}} = 0.40(4)$ [22], in good agreement with ideal LTO, signifying that the pristine samples are fully ordered [23]. For the irradiated samples, each irradiated sample intensity ratio, $I\{111\}/I\{222\}|_{\text{irradiated}}$, was divided by the measured pristine intensity ratio, $I\{111\}/I\{222\}|_{\text{pristine}}$, to obtain a *normalized* ratio (r in Table I). Using the calculated structure factors, a dependence of i on r was determined via a fit to the following (purely empirical) exponential/linear function: $i(r) = -0.020\,343\,9 + 0.522\,131 \exp(-r^{0.5}) - 0.173\,508r$. The "goodness of fit" of this equation is represented by a calculated chi-squared value of $\chi^2 = 1.0004$. This expression for $i(r)$ was used to convert the normalized intensity ratio, r, for each irradiated sample to an inversion value (Table I). The inversion values, i, in Table I were taken together with the lattice swelling values to reveal a quantitative relationship between swelling and cation inversion.

A key finding from the above analysis, shown in Fig. 2, is that for $i = 0.0625$, the lattice swelling is $\Delta V = 12 \pm 1$ Å^3 (indicated by thick lines in Fig. 2) [24]. (The estimated standard error is based on the errors associated with two data points, specifically, the pristine and 2×10^{18} Ne/m^2 data points.) An inversion of 0.0625 represents an antisite concentration equivalent to an average of one antisite pair per cubic unit cell (u.c.) [25]. Thus, if all of the swelling in LTO is due to antisite formation (and accompanying anion relaxations), then the volume per cation antisite pair is $V(\text{antisite pair}) \sim 12$ Å^3.

Atomistic calculations were performed to determine the volume swelling and energy associated with individual antisite defects. First, DFT calculations were performed on LTO, with and without incorporating one antisite pair into one unit cell of LTO, as a function of the separation of the antisite pair. It was found that there is no significant difference in behavior for antisites that are nearest neighbors and those separated as far apart as the computational cell allows (about 10 Å). Both the formation volumes (19.7 Å^3 for near-neighbor and 16.9 Å^3 for separated) and the formation energies (0.81 eV, near-neighbor and 0.85 eV, separated) of cation antisite pairs in LTO, relative to ordered pyrochlore, are very similar. DFT calculations also revealed that the oxygen sublattice is profoundly affected by the introduction of cation antisites into the pyrochlore lattice. Even the introduction of one antisite pair in the unit cell causes significant distortion of the oxygen sublattice, consistent with the DFT findings of Zhang *et al.* [26].

While the DFT calculated volumes for antisites (19.7 and 16.9 Å^3) do not agree exactly with the experimental volume of ~12 Å^3 per antisite pair, these calculated volumes are closer to experiment than calculated volumes for other possible lattice defects. Take, for instance, cation

TABLE I. Experimental results for lattice swelling (Δa and ΔV) and cation inversion (i) in LTO relative to the pristine sample, as a function of Ne ion irradiation fluence, based on GIXRD measurements. The surface and peak dpa are the displacement doses at the surface and the peak of the damage curve, as calculated with the SRIM.

Sample	Fluence Ne/m^2	Surface/Peak dpa	a(Å)	Δa(Å)	V(Å^3)	ΔV(Å^3)	$I\{111\}/I\{222\}$	r	$i(r)$
Pristine			9.999(6)		999.60(9)		0.40(4)	1.00(0)	0.00(0)
Irradiated	2×10^{18}	0.02/0.07	10.054(4)	0.055(8)	1016.(1)	17.0(11)	0.271(20)	0.68(9)	0.09(1)
Irradiated	5×10^{18}	0.05/0.2	10.059(3)	0.060(7)	1017.7(8)	18.1(9)	0.180(20)	0.45(7)	0.17(2)
Irradiated	7×10^{18}	0.07/0.25	10.084(5)	0.080(8)	1025.5(13)	26.0(10)	0.13(3)	0.32(9)	0.22(6)

Frenkel pairs. DFT indicates that the formation volume of a Ti Frenkel pair is 53.5 Å^3 and that of a Lu Frenkel pair is 49.7 Å^3. Any significant concentration of cation Frenkel pairs would produce swelling far in excess of the observed lattice swelling. Further, the energies of the Frenkel pairs are much higher than the antisite configurations: 3.3 and 2.8 eV for the Ti and Lu Frenkel pairs, respectively, vs 0.81 and 0.85 eV for near and far antisites, respectively.

Finally, it is natural to ask how the antisites form during the irradiation of the material. There are two possible mechanisms, directly in-cascade or via the thermal evolution of Frenkel pairs produced by cascades. To understand how Frenkel pairs might evolve, the kinetic evolution of single Frenkel pairs within LTO was investigated using TAD. As the interstitial component of the Frenkel pair diffuses towards the vacancy, instead of perfect recombination of these defects, antisite pairs are always produced in TAD simulations [Fig. 3(a)]. In fact, at times, multiple antisites can be produced from one Frenkel pair [Fig. 3(b)]. This occurs for both cation species. The reason for this is that, because the interstitial diffuses via an interstitialcy mechanism (pushing out a lattice ion as it diffuses), as it approaches the vacancy, it cannot simply hop to fill the vacancy. Rather, it pushes out the cation closest to the vacancy, which is always a cation of the opposite species (for $i \sim 0$). This cation falls into the vacancy, creating the antisite pair. Thus, while Frenkel pairs are created during damage events, they are only metastable and eventually decay to antisites. This behavior is similar to that seen by Devanathan *et al.* [27] and Chartier *et al.* [28], though in those cases, the antisites formed from the recombination of close Frenkel pairs. However, the barriers for the Frenkel pair decay processes found in our study, predicted by the potential and validated with DFT, are quite high (1–2 eV) and would not be thermally active at 77 K. Thus, we conclude that the formation of antisites, observed in the experiment, must occur "in-cascade," as energetic displaced atoms thermalize following cascade events. Our atomistic simulations also reveal that the barriers are much higher for neighboring antisites to annihilate and produce a perfect crystal (> 10 eV), meaning that once they form, they will be stable for extremely long times. The TAD and prior MD simulations [27,28] reveal that while ordered pyrochlore is the preferred thermodynamic state of the material, kinetics prevent this state from being reached—perfect recombination is extremely unlikely and cation lattice disorder will be the *de facto* consequence of irradiation.

Thus, we have three pieces of evidence that lead us to conclude that the defects responsible for swelling in LTO are antisites and they are formed directly in cascades: (1) the measured changes in structure factors as a function of irradiation are consistent with a defect that remains on the fluorite lattice, suggesting antisites as opposed to interstitials; (2) formation volumes of defects in LTO, calculated with DFT, show that antisites have a volume most consistent with experimental measurements; and (3) TAD simulations show that Frenkel pairs are at best metastable but that the barriers for forming antisites are very high, suggesting antisites form in collision cascades directly. Independently, none of these results would be conclusive. But collectively, these three results strongly

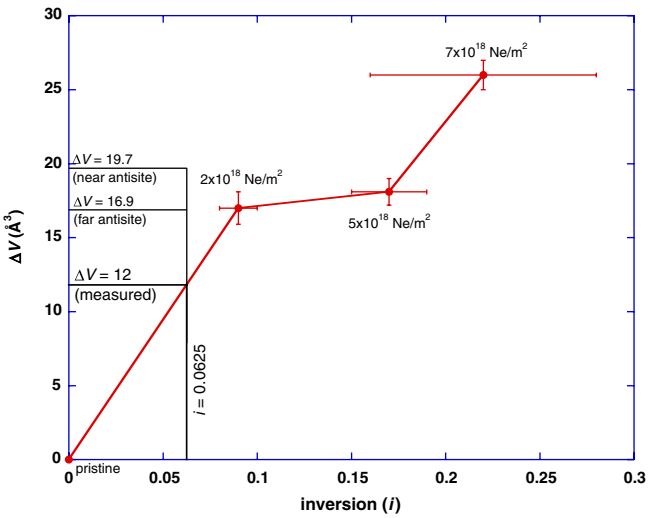

FIG. 2 (color online). Unit cell swelling (ΔV) versus cation inversion (i), based on the GIXRD patterns in Fig. 1 (see text for discussion). The thick solid lines indicate the estimated swelling (12 Å^3) associated with the introduction of a single cation antisite pair ($i = 0.0625$) into one unit cell in $Lu_2Ti_2O_7$. Theoretically predicted formation volumes for cation antisite defects are shown as horizontal thin solid lines: (1) a distant antisite pair ($\Delta V = 16.9$ Å^3); and (2) a near-neighbor antisite pair ($\Delta V = 19.7$ Å^3). The errors are standard errors of the fitted unit cell volumes (ordinate) and the fitted x-ray peak intensities (along with conversion to an inversion parameter, i) (abscissa).

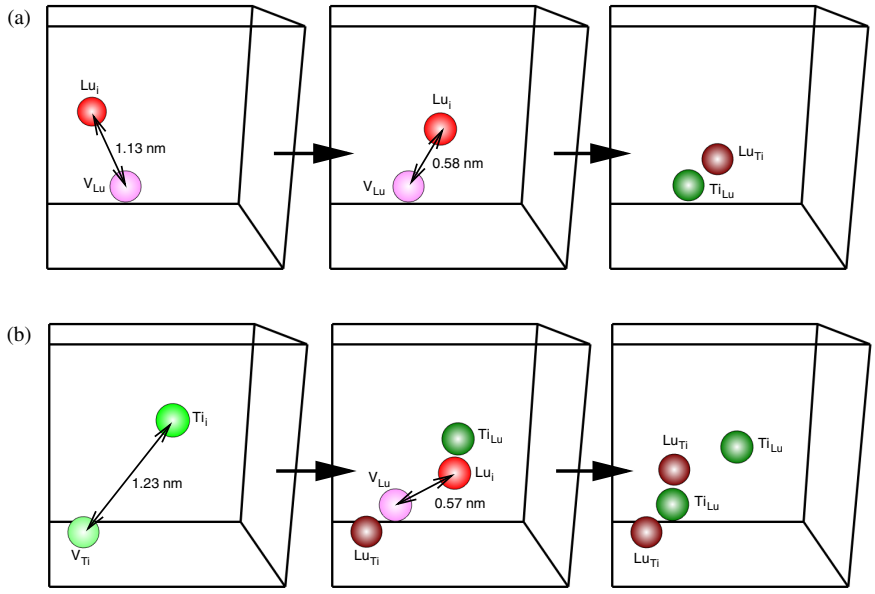

FIG. 3 (color online). Frames from temperature accelerated dynamics simulations showing the evolution of point defects in $Lu_2Ti_2O_7$. (a) Lu Frenkel pair ($Lu_i + V_{Lu}$). The Lu_i and V_{Lu} point defects migrate towards one another, but rather than annihilating to produce a perfect crystal, they decay into a near-neighbor antisite pair ($Lu_{Ti} + Ti_{Lu}$). (b) Ti Frenkel pair ($Ti_i + V_{Ti}$). The Ti_i does not migrate, but instead decays into the defect pair, $Lu_i + Ti_{Lu}$. V_{Ti} also decays during migration into an additional defect pair, $V_{Lu} + Lu_{Ti}$. The $Lu_i + V_{Lu}$ defects then react as in (a), leaving two antisite pairs ($Lu_{Ti} + Ti_{Lu}$).

support the conclusion that titanate pyrochlores experience significant radiation-induced cation disordering, leading to substantial lattice swelling at low displacement damage doses.

Previously, we reported that titanate pyrochlores ($Ln_2Ti_2O_7$) are far more susceptible to radiation-induced amorphization than are zirconates ($Ln_2Zr_2O_7$) [29,30]. We concluded that this is because zirconates can more readily accommodate disorder (especially antisites) than can titanates. However, the study presented here demonstrates that though disorder in titanates is energetically costly [29], they still succumb to significant lattice disorder under irradiation, even at low dose. This disorder increases with dose and is ultimately responsible for their amorphization.

One additional observation is worthy of note. Figure 1 shows that the Bragg diffraction maxima broaden with increasing ion fluence. Moreover, this peak broadening is approximately symmetric. Symmetric peak broadening usually indicates positive and negative strain from defects; for instance, interstitials and vacancies can produce this effect [31]. Similarly, if cation antisite pairs are produced by irradiation (as we postulate), then one antisite, say A_B, should induce positive strain, while the other antisite, B_A, induces negative strain. Indeed, this is what we find using DFT. In LTO, isolated Lu_{Ti} and Ti_{Lu} antisites produce calculated strains of $+21.7$ and -1.8 Å^3, respectively, the sum of which (19.9 Å^3) is close to the other calculations described above (19.7 and 16.9 Å^3 for near and distant cation antisite pairs, respectively). While this does not prove we have cation antisites, it is yet another result that is consistent with our interpretation that the principal radiation-induced defects are cation antisite pairs.

In summary, x-ray diffraction was used to quantify the nature of irradiation-induced lattice swelling in a complex oxide, $Lu_2Ti_2O_7$, following 400 keV Ne ion irradiation at cryogenic temperature. The swelling was determined to be due to cation antisite defects ($Lu_{Ti} + Ti_{Lu}$). In addition, experimental results indicate that the volume change associated with a single antisite pair in a unit cell is approximately 12 Å^3. First principles calculations found that the volumes of antisite pairs (19.7 Å^3 near-neighbor and 16.9 Å^3 separated) agree much better with experiment than other candidate defects such as cation Frenkel pairs. Moreover, temperature accelerated dynamics simulations indicate that cation Frenkel defects require long times to decay to form cation antisite pairs, suggesting that antisites are formed directly in cascades. Taking all of these results together, the implication is that irradiation-induced lattice swelling in $Lu_2Ti_2O_7$ is due primarily to $Lu_{Ti} + Ti_{Lu}$ antisites. Other $Ln_2Ti_2O_7$ pyrochlores with even larger Ln^{3+} cations than Lu^{3+}, show similar behavior (experimental results not reported here).

The quantification of the properties of cation antisite defects achieved here has implications not only for radiation damage effects in complex oxides, but also for oxygen transport in solid oxide fuel cells [32,33] and for thermal transport in inert matrix fuels [34] and thermal barrier coatings [35].

The authors acknowledge support provided by the DOE Office of Basic Energy Sciences (OBES), Division of

Materials Sciences. Y. H. Li was partially supported by the National Natural Science Foundation of China (11175076, 10975065). Discussions with Dr. J. P. Hirth, Dr. T. E. Mitchell, and Dr. M. F. Fitzsimmons are gratefully acknowledged.

*kurt@utk.edu

[1] W. J. Weber, J. Am. Ceram. Soc. **65**, 544 (1982).
[2] C. H. Johansson and J. O. Linde, Ann. Phys. (Leipzig) **417**, 1 (1936).
[3] A. V. Shlyakhtina, L. G. Shcherbakova, and A. V. Knot'ko, Russ. J. Electrochem. **39**, 467 (2003).
[4] A. V. Shlyakhtina, L. G. Shcherbakova, and A. V. Knotko, Ferroelectrics **294**, 175 (2003).
[5] A. V. Shlyakhtina, L. G. Shcherbakova, A. V. Knotko, and A. V. Steblevskii, J. Solid State Electrochem. **8**, 661 (2004).
[6] K. B. Helean, S. V. Ushakov, C. E. Brown, A. Navrotsky, J. Lian, R. C. Ewing, J. M. Farmer, and L. A. Boatner, J. Solid State Chem. **177**, 1858 (2004).
[7] A. V. Shlyakhtina, A. E. Ukshe, and L. G. Shcherbakova, Russ. J. Electrochem. **41**, 265 (2005).
[8] B. D. Begg, N. J. Hess, W. J. Weber, R Devanathan, J. P. Icenhower, S. Thevuthasan, and B. P McGrail, J. Nucl. Mater. **288**, 208 (2001).
[9] J. Lian, L. Wang, J. Chen, K. Sun, R. C. Ewing, J. M. Farmer, and L. A. Boatner, Acta Mater. **51**, 1493 (2003).
[10] J. F. Ziegler, J. P. Biersack, and U. Littmark, *The Stopping and Range of Ions in Solids* (Pergamon Press, New York, 1985), Vol. 1, p. 321.
[11] A. J. C. Wilson and E. Prince, *International Tables for Crystallography: Volume C-Mathematical, Physical and Chemical Tables* (Kluwer Academic Publishers, Dordrecht/Boston/London, 1999), Vol. C, p. 992.
[12] G. Kresse and J. Hafner, Phys. Rev. B **48**, 13115 (1993).
[13] G. Kresse and J. Furthmuller, Comput. Mater. Sci. **6**, 15 (1996).
[14] G. Kresse and J. Furthmuller, Phys. Rev. B **54**, 11169 (1996).
[15] G. Kresse and D. Joubert, Phys. Rev. B **59**, 1758 (1999).
[16] M. R. Sorensen and A. F. Voter, J. Chem. Phys. **112**, 9599 (2000).
[17] L. Minervini, M. O. Zacate, and R. W. Grimes, Solid State Ionics **116**, 339 (1999).
[18] L. Minervini, R. W. Grimes, and K. E. Sickafus, J. Am. Ceram. Soc. **83**, 1873 (2000).
[19] In a complex oxide with equal proportions of two cations, *superlattice* reflections scale as $(f_A - f_B)^2$, where f_A and f_B are atomic form factors for A and B cations. On the other hand, *fundamental* reflections scale as $(f_A + f_B)^2$. As antisite defects accumulate, superlattice reflections diminish in intensity, while fundamental reflections remain unchanged.
[20] Other defects formed under irradiation have distinctly different effects on the relative intensities of Bragg diffraction maxima. For instance, a cation vacancy removes scattering power from the structure factors of allowed reflections, but the net effect on intensities is to diminish the fundamental reflections while increasing the intensities of the superlattice reflections (N.B.: some reflections are due only to anion arrangements, e.g., {220} and {422}; these are unaffected by cation vacancies).
[21] See Supplemental Material at http://link.aps.org/supplemental/10.1103/PhysRevLett.108.195504 for detailed descriptions of: lattice volume calculations; cation inversion calculations; ion irradiation induced lattice strains; irradiation-induced amorphization transformations; implanted ion concentrations; and DFT calculations.
[22] The error is based on several measurements of different pristine samples mounted in various orientations on the GIXRD diffractometer. That the error in $I\{111\}/I\{222\}|_{\text{pristine}}$ is relatively small ($\pm$ 0.04) suggests that there is little or no texture in the as-fabricated LTO samples.
[23] This was confirmed by powder x-ray diffraction (XRD) measurements on the identical, pristine LTO material. Rietveld refinements of the powder XRD data indicate that the pristine LTO samples possess fully ordered cation sublattices.
[24] The antisite pair defect volume shown in Fig. 2 was estimated using only the pristine and 2×10^{18} Ne/m^2 data points as the errors are relatively small for these two data points. The error in the inversion becomes very large at 7×10^{18} Ne/m^2. This is because the {111} peak becomes quite small relative to the background by this fluence.
[25] The peak displacement dose at $i = 0.0625$ is estimated to be 0.045 displacements per atom (dpa), or 4 point defects per u.c. (one u.c. contains 88 atoms). One antisite pair per u.c. is equivalent to 2 displacements per 88 atoms or 0.023 dpa.
[26] Z. L. Zhang, H. Y. Xiao, X. T. Zu, F. Gao, and W. J. Weber, J. Mater. Res. **24**, 1335 (2009).
[27] R. Devanathan, W. J. Weber, and J. D. Gale, Energy Environ. Sci. **3**, 1551 (2010).
[28] A. Chartier, G. Catillon, and J. P. Crocombette, Phys. Rev. Lett. **102**, 155503 (2009).
[29] K. E. Sickafus, L. Minervini, R. W. Grimes, J. A. Valdez, M. Ishimaru, F. Li, K. J. McClellan, and T. Hartmann, Science **289**, 748 (2000).
[30] K. E. Sickafus, R. W. Grimes, J. A. Valdez, A. Cleave, M. Tang, M. Ishimaru, S. M. Corish, C. R. Stanek, and B. P. Uberuaga, Nature Mater. **6**, 217 (2007).
[31] B. C. Larson, in *Diffuse Scattering and the Fundamental Properties of Materials*, edited by R. I. Barabash, G. E. Ice, and P. E. A. Turchi (Momentum Press, New York, NY, 2009), pp. 139.
[32] P. J. Wilde and C. R. A. Catlow, Solid State Ionics **112**, 173 (1998).
[33] P. J. Wilde and C. R. A. Catlow, Solid State Ionics **112**, 185 (1998).
[34] P. Shukla, A. Chernatynskiy, J. C. Nino, S. B. Sinnott, and S. R. Phillpot, J. Mater. Sci. **46**, 55 (2011).
[35] P. K. Schelling, S. R. Phillpot, and R. W. Grimes, Philos. Mag. Lett. **84**, 127 (2004).